Anxiogenic and Stressor Effects of the Hypothalamic Neuropeptide RFRP-3 Are Overcome by the NPFFR Antagonist GJ14

Joon S. Kim, Phil W. Brownjohn, Blake S. Dyer, Massimiliano Beltramo, Christopher S. Walker, Debbie L. Hay, Gavin F. Painter, Joel D. A. Tyndall, and Greg M. Anderson

Centre for Neuroendocrinology and Department of Anatomy (J.S.K., P.W.B., G.M.A.) and National School of Pharmacy (J.D.A.T.), University of Otago, Dunedin 9054, New Zealand; Glycosyn (B.S.D.), Callaghan Innovation (B.S.D.), and The Ferrier Research Institute (G.F.P.), University of Wellington, Lower Hutt 5010, Victoria, New Zealand; Institut National de la Recherche Agronomique (M.B.), Nouzilly 37380, France; and School of Biological Sciences (C.S.W., D.L.H.), University of Auckland, Auckland 1142, New Zealand

RFamide-related peptide-3 (RFRP-3) is a recently discovered neuropeptide that has been proposed to play a role in the stress response. We aimed to elucidate the role of RFRP-3 and its receptor, neuropeptide FF (NPFF1R), in modulation of stress and anxiety responses. To achieve this, we characterized a new NPFF1R antagonist because our results showed that the only commercially available putative antagonist, RF9, is in fact an agonist at both NPFF1R and the kisspeptin receptor (KISS1R). We report here the identification and pharmacological characterization of GJ14, a true NPFFR antagonist. In in vivo tests of hypothalamic-pituitary-adrenal (HPA) axis function, GJ14 completely blocked RFRP-3-induced corticosterone release and neuronal activation in CRH neurons. Furthermore, chronic infusion of GJ14 led to anxiolytic-like behavior, whereas RFRP-3 infusion had anxiogenic effects. Mice receiving chronic RFRP-3 infusion also had higher basal circulating corticosterone levels. These results indicate a stimulatory action of RFRP-3 on the HPA axis, consistent with the dense expression of NPFF1R in the vicinity of CRH neurons. Importantly, coinfusion of RFRP-3 and GJ14 completely reversed the anxiogenic and HPA axis-stimulatory effects of RFRP-3. Here we have established the role of RFRP-3 as a regulator of stress and anxiety. We also show that GJ14 can reverse the effects of RFRP-3 both in vitro and in vivo. Infusion of GJ14 causes anxiolysis, revealing a novel potential target for treating anxiety disorders. (*Endocrinology* 156: 4152–4162, 2015)

The G-protein coupled neuropeptide FF (NPFF) receptors belong to the RFamide receptor family and are referred to as NPFF1R (also known as GPR147) and NPFF2R (GPR74). The endogenous ligands, RFamide related peptide-3 (RFRP-3; also known as gonadotrophin inhibitory hormone) and NPFF, display high affinity to both receptors while preferentially activating NPFF1R and NPFF2R, respectively (1, 2). RFRP-3 is a neuropeptide first described in birds as a putative gonadotropin inhibitory hormone for its inhibitory effects on the reproductive axis (3, 4). In mammals, the significance of this inhibitory role of RFRP-3 has been inferred in part from the effects of RF9, a putative NPFF receptor antagonist. RF9 induces a remarkably potent gonadotropin release (5–10), which has been interpreted as RFRP-3 having a very potent tonic inhibitory action on the GnRH neurons, which drive gonadotropin release.

Beyond the reproductive axis, RFRP-3 has also recently been shown to be up-regulated by restraint stress in male and female rodents, perhaps as a mechanism of stress-

ISSN Print 0013-7227 ISSN Online 1945-7170
Printed in USA

Received June 15, 2015. Accepted August 4, 2015.
First Published Online August 10, 2015

Abbreviations: GFP, green fluorescent protein; HEK, human embryonic kidney; HPA, hypothalamic-pituitary adrenal; i.c.v., intracerebroventricular; IP1, inositol phosphate 1; KISS1R, kisspeptin receptor; NPFF, neuropeptide FF; NPFF1R, neuropeptide FF receptor 1; NPFF2R, neuropeptide FF receptor 2; NPY, neuropeptide Y; NPY-Y1, Neuropeptide Y receptor 1; PVN, paraventricular nucleus; RFRP-3, RFamide related peptide-3.

induced infertility (11, 12). Given the widespread projections of RFRP-3 fibers and the dense expression of NPFF1R in the paraventricular nucleus (PVN), in the basolateral amygdala, in the lateral septum, and throughout the limbic system, it is likely that RFRP-3 has other roles in stress modulation that are yet to be elucidated (1, 10, 13). The stress-induced activation of the hypothalamic-pituitary adrenal (HPA) axis is dependent on CRH neurons in the PVN, which stimulate the release of adrenocorticotropic hormone from the anterior pituitary gland. This in turn stimulates the production of adrenal stress hormones (14). The afferent inputs that modulate CRH neuronal tone and its interaction with cognitive processing centers such as the limbic system remain poorly characterized. In addition to regulating the stress response, there is good preclinical and clinical evidence to support the role of CRH in the underlying mechanisms of anxiety (15–17). CRH receptor antagonists (18) and CRH receptor-null mice (19, 20) both consistently report an anxiolytic-like effect in the literature. Therefore, pharmacological manipulation of CRH neuron excitability via upstream targets may provide treatment targets for anxiety and stress-related disorders.

Evidence from rats suggests that treatment with RFRP-3 may promote stress responses (21). In part, the lack of a useful receptor antagonist has made it difficult to advance the understanding of this and other roles of RFRP-3. Whereas RF9 is claimed to be a highly specific and potent NPFF receptor antagonist (22), there have been recent suggestions that RF9 has off-target actions (23) and may even be an agonist at NPFF1R (24, 25). We describe here the identification of a highly specific and potent NPFF1R antagonist with moderate antagonism at NPFF2R, named GJ14 (Figure 1). We also show that RFRP-3 alone is both an activator of the HPA axis and an anxiogenic neuropeptide in mice. Infusion of GJ14 blocks this effect and causes anxiolysis, revealing a novel potential target for treating anxiety disorders.

Materials and Methods

Materials

For in vitro experiments, RF9 was purchased from Tocris Biosciences. Human NPFF and human RFRP3 were purchased from Phoenix Pharmaceuticals and Bachem, respectively. Human kisspeptin-10 and human neuropeptide Y (NPY) were purchased from Calbiochem. For in vivo experiments, rat RFRP-3 was purchased from Bachem.

Drug design

Eight peptidic compounds were generated based on RF9 (22), the NPY-Y1/NPFFR antagonist BIBP3226 (26), and its derivatives (27, 28) (Figure 1). The rationale was to vary either the hydrophobic N-terminal group (diphenyl, adamantly, or dansyl), the C-terminal group based on phenylalanine-amide (phenylglycine with or without the amide), and the stereochemistry of the original amino-acid centers. Details of drug synthesis and analysis are described in Supplemental Materials and Methods.

In vitro experiments

Cell culture

Chinese hamster ovary (CHO-K1) cells stably transfected with human NPFF1R/Gα15 (GenScript), human NPFF2R (28, 29) (a gift from Catherine Mollereau, Centre National de la Recherche Scientifique, Universite de Toulouse, France), or human NPY-Y1 (PerkinElmer) and human embryonic kidney (HEK)-293 cells transfected with human kisspeptin receptor (KISS1R) (30) (a gift from Nicolas de Roux, Robert Debré Hospital, Paris, France) were used for radioligand binding and second messenger experiments. Gα15 is a promiscuous Gq protein and allows the NPFF1R receptor to signal via both Gi and Gq pathways when activated.

Experiment 1a: radioligand binding

Cells were harvested at approximately 80% confluence and underwent a series of homogenization and ultracentrifugation

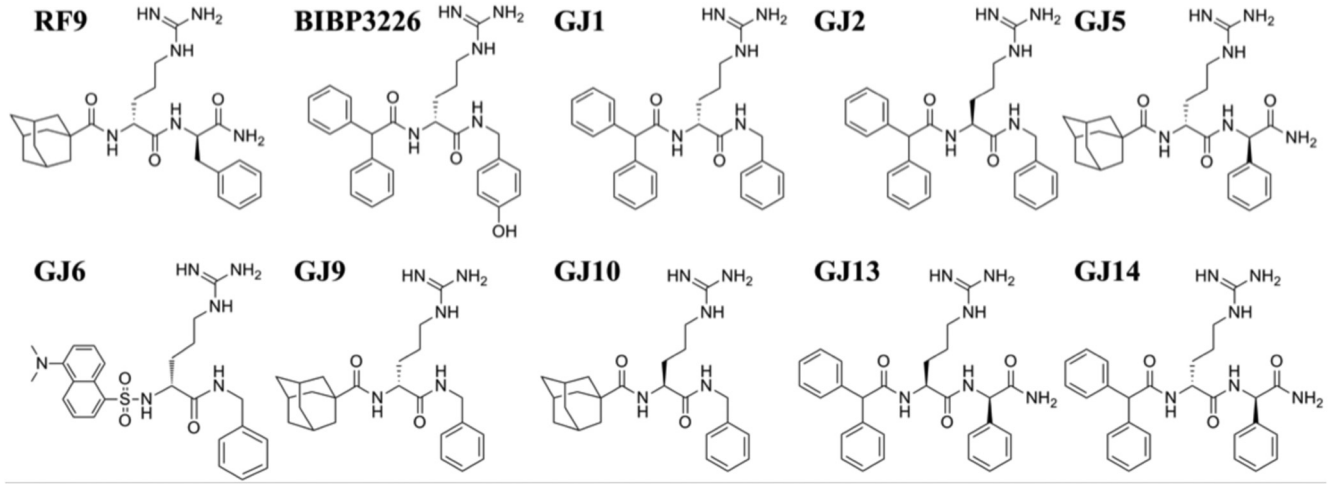

Figure 1. Compound structures of RF9, BIBP3226, and eight test compounds.

steps to generate a membrane-rich homogenate. For competitive binding assays, membranes-rich homogenate was incubated in a 96-well plate with the appropriate ^{125}I-labeled ligand (all purchased from PerkinElmer) and increasing concentrations of the test compounds. ^{125}I-NPFF (catalog number NEX381) was used to bind both NPFF receptor subtypes; ^{125}I-peptide YY (NEX381) was used to bind NPY-Y1 and ^{125}I-kisspeptin-10 (NEX395) was used to bind KISS1R. The reaction was terminated by rapid filtration using a cell harvester, and the filter-bound radioactivity was measured using a γ-counter. The concentration of the radioligand (approximately equal to the kilodalton) was predetermined from a saturation binding assay (data not shown). Details of the competitive binding experiments and buffers used are described in the Supplemental Materials and Methods.

Experiment 1b: cellular assays

For Gi-coupled receptors (NPFF1R, NPFF2R, NPY-Y1), the peptidic compounds were used to block the agonist-induced 3′,5′-cAMP inhibition (LANCE Ultra cAMP assay kit; PerkinElmer). For receptor stimulation assays, forskolin was used to stimulate endogenous cAMP production, which was then inhibited by known endogenous agonists or test compounds. Agonism was measured by the inhibition of forskolin-induced cAMP production. For antagonism assays, the test compounds were added in the presence of both forskolin and the endogenous agonist. For the Gq-coupled KISS1R, the accumulation of inositol phosphate 1 (IP1) was measured (IP-One HTRF kit; Cisbio Assays). For receptor stimulation assays, the test compounds were tested alone and agonism was measured by the accumulation of IP1. For antagonism assays, the test compounds were tested in the presence of the endogenous agonist, kisspeptin. All second-messenger assays were performed in 384-well plates according to the manufacturers' instructions and read using an Envision plate reader (PerkinElmer). Calcium levels were measured in the NPFF1R cell line, using a FLIPR Calcium 4 assay kit (Molecular Devices) according to the manufacturer's instructions and read using a Victor X3 plate reader (PerkinElmer). Details of the cellular assay experiments and buffers used are described in Supplemental Materials and Methods.

Data analysis

Data were analyzed using GraphPad Prism 6 (GraphPad Software). For agonist curves, EC_{50} and IC_{50} values were obtained by fitting a four-parameter logistic equation. F tests were performed to determine whether the Hill slope was significantly different from 1. When the Hill slope was not significantly different from unity, curves were refitted with a Hill slope constrained to 1. For antagonist potency, curves were fitted using the Gaddum/Schild EC_{50} shift equation and pA_2 values determined.. F tests were performed within each individual data set to confirm antagonism by determining whether a single curve adequately fit both the agonist and antagonist shifted data. For analysis pIC_{50}, pEC_{50} and pA_2 values were combined from individual experiments. All data are reported as mean ± SEM.

In vivo experiments

Animals

All mice were housed in individually ventilated cages under conditions of controlled lighting (lights on at 8:00 AM, lights off at 8:00 PM) with ad libitum access to standard chow and water. All in vivo experiments were approved by the University of Otago Animal Ethics Committee.

Experiment 2: LH responses to RF9 and GJ14

To determine the estrous cycle stage, 7- to 10-week-old female C57BL/6 mice were monitored by vaginal lavage and cytology daily for at least 4 days leading up to the time of experiment. Between 10:00 AM and 1:00 PM, diestrous mice were blood sampled (5 μL) from the tail tip and then given an injection of RF9 (4 or 8 nmol/mouse), GJ14 (8 nmol/mouse), or saline vehicle into the left lateral ventricle under brief isoflurane anesthesia. Mice were returned to their cages, and repeated tail blood samples were obtained and assayed for whole-blood LH concentration by an ELISA (31). A group of 7- to 10-week-old 129S6/Sv/Ev KISS1R knockout (KISS1R KO) female mice and their littermate wild-type controls were included to test whether the response to RF9 involved the kisspeptin receptor. These mice were pretreated with four priming injections of GnRH (4 nmol/kg, sc) spaced 4 hours apart with the last injection given 3 hours prior to RF9 treatment (8 nmol/mouse). This protocol allows the pituitary gland to become more responsive to GnRH in this mouse line as previously reported (32). In a separate study, we showed that these injections caused a robust 2.5-fold increase in basal circulating LH concentration, regardless of genotype (data not shown). The LH assay sensitivity was 0.15 ng/mL and the mean intra- and interassay coefficients of variation were 7.2% and 5.8%, respectively.

Experiment 3: corticosterone measurements and HPA axis activation

Male transgenic C57BL/6 background *Crh*-Cre (33) X *Tau*-green fluorescent protein (GFP) mice (henceforth referred to as CRH-GFP mice) were used to visualize hypothalamic CRH neurons. This *Crh*-Cre mouse line has been extensively characterized and reliably reports Cre expression in essentially all CRH neurons (34). Between 8:00 AM and 1:00 PM, 10-week-old CRH-GFP male mice were anesthetized and implanted with a 26-gauge guide cannula (number C315GS-2/SPC; Plastics One Inc) into the left lateral ventricle. The guide cannulae were anchored to the skull using dental cement. After 6 days, conscious mice were given intracerebroventricular (i.c.v.) injections of RFRP-3 (3 nmol/mouse), GJ14 (30 nmol/mouse), RFRP-3 + GJ-P14, or vehicle using a Hamilton syringe. All injections were administered in 1 μL over a 1-minute duration. Handling control mice received brief restraint only. Untreated mice were immediately decapitated to show basal corticosterone levels. Mice were decapitated 35 minutes after injection and trunk blood samples and brains were collected. Serum corticosterone was measured using an ELISA (Arbor Assays). The assay sensitivity was 22.2 pg/mL and the mean intra- and interassay coefficients of variation were 4.2% and 3.4%, respectively. Brains were postfixed for 4 days in 4% paraformaldehyde, sliced into 30-μm coronal slices, and dual stained for GFP (chicken anti-GFP, number GFP-1020; Aves Labs; 1:2500) and cFOS (a marker of neuronal activation, AB-5 PC38; Calbiochem; 1:10 000) (Table 1). Primary antibodies were visualized using Alexa Fluor 488 goat antichicken IgG (1:500; Molecular Probes, Life Technologies) and Alexa Fluor 568 goat antirabbit (1:500). Sections were photographed under

Table 1. Antibody Table

Peptide/Protein Target	Antigen Sequence (if Known)	Name of Antibody	Manufacturer, Catalog Number, and/or Name of Individual Providing the Antibody	Species Raised (Monoclonal or Polyclonal)	Dilution Used
GFP	N/A	Green fluorescent protein	Aves Labs, number GFP-1020	Chicken polyclonal	1:25 000
cFOS	SGFNADYEASSSRC	Anti-cFos (AB-5) (4–17) rabbit pAb	Calbiochem, PC38	Rabbit polyclonal	1:10 000
Chicken IgG		Alexa Fluor 488 conjugate IgG	Invitrogen	Goat	1:500
Rabbit IgG		Alexa Fluor 568 conjugate IgG	Invitrogen	Goat	1:500

confocal microscopy (Zeiss LSM 710). Omission of primary antibody resulted in no staining.

Experiment 4: anxiety behavior testing

Female C57BL/6 mice (8 wk old) were given i.c.v. implants connected to an osmotic minipump (Alzet model 1007D; Durect Corp), delivering 0.5 μL/h of vehicle, RFRP-3 (2 nmol/mouse/d), GJ14 (20 nmol/mouse/d), or RFRP-3+GJ14 into the left lateral ventricle. On the fifth day of infusion, the mice were subjected to behavioral testing. All behavioral testing took place between 8:00 AM and 1:00 PM. Mice were exposed to the elevated plus maze and open field tests for 5 minutes each. For the light dark box, the test was 10 minutes in duration. These times were based on pilot experiments (data not shown). To avoid exposure to multiple sequential testing paradigms, two sets of experiments were conducted. The first set of mice was tested on the elevated plus maze, immediately followed by the open field. The second set of mice was tested in the light dark box and mice were returned to their cages for 3 hours. After this testing, the mice were decapitated and trunk blood was collected for a corticosterone ELISA. Except for the sequence of testing described above, mice were naïve to the tests at the time of experimentation.

Data analysis

Statistical analyses were carried out using GraphPad Prism 6. Values are reported as mean ± SEM. Statistical analysis was performed using a one-way ANOVA (with post hoc Tukey's multiple comparisons test). Repeated LH measurements were assessed using a two-way, repeated-measures ANOVA (with sampling time and treatment group as the factors and post hoc Bonferroni test).

Results

Experiment 1a and b: pharmacological characterization of antagonists

The binding affinities of test compounds and reference ligands were initially tested on NPFF1R and NPFF2R (Figure 2, A and B) as well as the related receptors NPY-Y1 and KISS1R (Supplemental Table 1). GJ14 displayed the highest affinity for both NPFF receptor subtypes of any non-endogenous compounds, surpassing that of RF9 by a 10-fold magnitude on NPFF1R (Table 2). GJ14 had higher affinity for NPFF1R over NPFF2R. Based on these results, GJ14 and GJ9, along with RF9, were selected for further functional experiments (results summarized in Table 2). Both RFRP-3 and NPFF inhibited forskolin-induced cAMP production at NPFF1R and NPFF2R (Figure 2, C and D), consistent with their known agonism at both receptor subtypes (1, 28). When tested alone, GJ14 and GJ9 had no effect on forskolin-induced cAMP levels at either NPFF receptors (Figure 2, C and D), whereas RF9 behaved as a full agonist at NPFF1R (EC_{50}; 1.16 μM, n = 3) (Figure 2C). The compounds were then used to concentration dependently block RFRP-3- or NPFF-induced cAMP inhibition at NPFF1R and NPFF2R, respectively (Figure 2, E and F). GJ14 (IC_{50}; 21.08 nM, n = 3) and GJ9 (IC_{50}; 210.75 nM, n = 3) were able to concentration dependently and completely block the effects of RFRP-3. In contrast, RF9 failed to antagonize the effect of RFRP-3 due to its agonism at NPFF1R (antagonist curve could not be generated; IC_{50} N.D., n = 3). GJ14, GJ9, and RF9 were able to completely block NPFF's agonism at NPFF2R, with near identical potency (Figure 2F).

To further confirm the antagonist activity of GJ14 and GJ9, we next generated concentration response curves for RFRP-3 and NPFF in the presence of a high concentration of the compounds (Figure 2, G and H). GJ14 (10 μM) and GJ9 (10 μM) shifted the concentration response curve of RFRP-3 to the right by 160-fold (pA_2; 7.25, n = 3) and 27-fold (pA_2; 6.34, n = 3). RF9 was used at 5 μM as pilot experiments showed RF9 has full agonistic properties at 10 μM, whereas at 1 μM, RF9 did not shift the RFRP-3 EC_{50} at 1 μM (data not shown). At the 5 μM concentration, RF9 behaved as a partial agonist and showed negligible antagonism of RFRP-3 (4-fold shift. pA_2; 5.75, n = 3). Statistical analysis of these data showed that GJ14 and GJ9 are significantly more effective antagonists of NPFF1R, compared with RF9 ($P < .001$ and $P < .05$, respectively, vs RF9 by a one way ANOVA followed by Dunnett's test). The compounds GJ14 (10 μM), GJ9 (10 μM), and RF9 (10 μM) once again showed virtually equipotent antagonistic properties at NPFF2R, shifting the NPFF EC_{50} by 12-fold, 10-fold, and 6-fold, respectively. These results confirmed that GJ14 is a potent NPFF1R antagonist with weak antagonism at NPFF2R, making it a suitable antagonist for blocking the effects of RFRP-3. GJ14 and GJ9 are significantly more effective antagonists

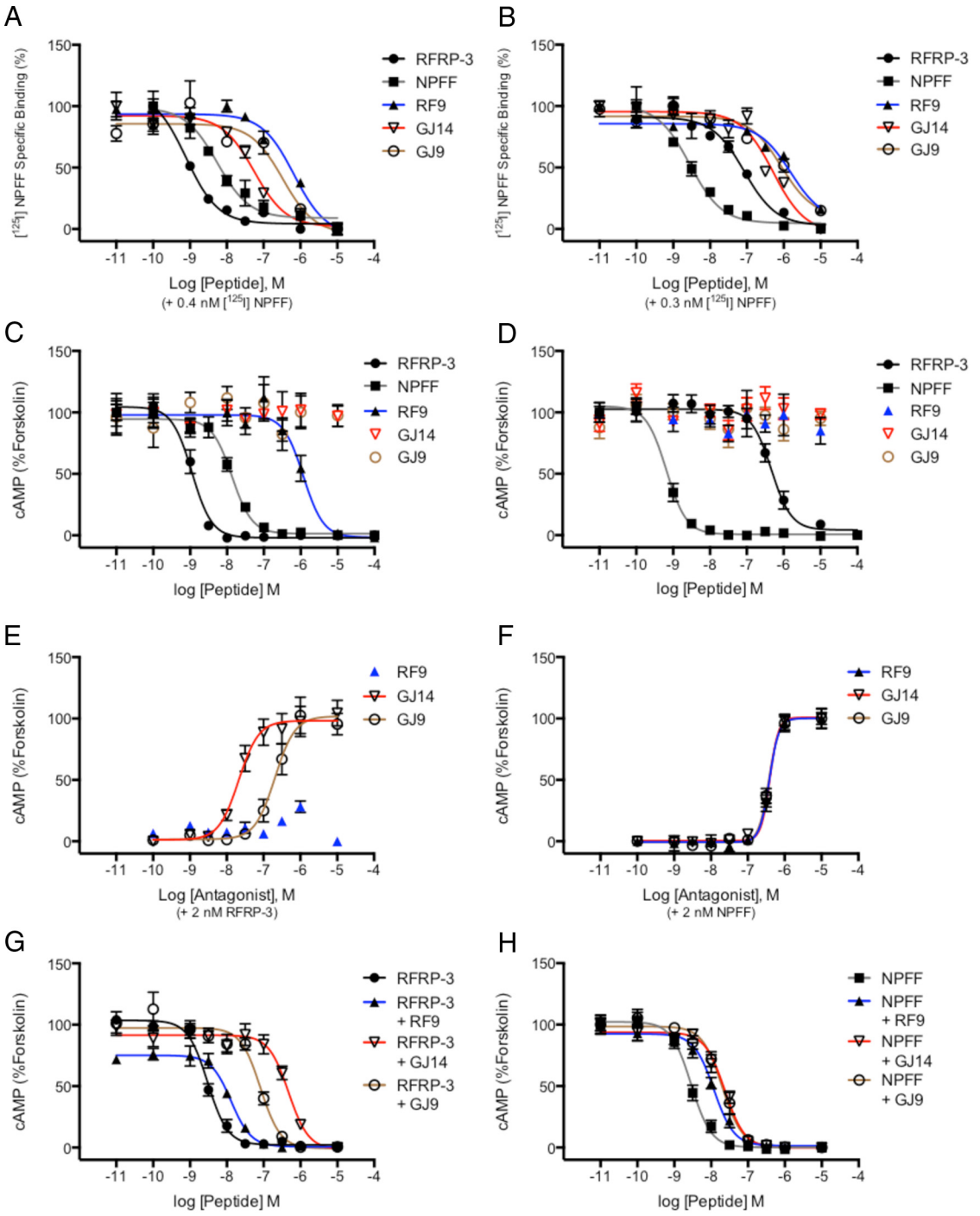

Figure 2. Pharmacology of test compounds (experiment 1a and 1b). Competitive displacement of [$^{[1125]}$]NPFF binding profiles of representative ligands and test compounds at NPFF1R (A) and NPFF2R (B). Effects of test compounds and ligands on forskolin-induced cAMP for NPFF1R- (C) and NPFF2R (D)-transfected CHO-K1 cells are shown. Antagonist-induced reversal of the agonist-induced cAMP inhibition for NPFF1R (E) and NPFF2R (F) are also shown. Agonist-induced inhibition of forskolin-induced cAMP production were performed alone or in the presence of antagonists at NPFF1R (G) and NPFF2R (H).

of NPFF1R than NPFF2R (GJ14, $P < .001$, NPFF1R vs NPFF2R; GJ9, $P < .05$, NPFF1R vs NPFF2R, both by unpaired t test). Furthermore, we report that in contrast to previous data, the putative NPFFR antagonist RF9 is a full NPFF1R agonist (22). Complementary to this, RF9 was also unable to block RFRP-3 induced calcium mobilization and showed agonistic properties when tested on the NPFF1R cell line (Supplemental Figure 1).

Off-target actions on the related receptors NPY-Y1 and KISS1R are summarized in Supplemental Table 1. In contrast to GJ1 and GJ2, GJ14, GJ9, and RF9 displayed no competitive displacement of ^{125}I-peptide YY at NPY-Y1 and furthermore

Table 2. Summary of the Pharmacology

	NPFF1R				NPFF2R			
Ligand	EC_{50}, nM[a]	IC_{50} (nM)[b]	EC_{50} Shift x-Fold[c]	pA_2[d]	EC_{50}, nM[a]	IC_{50}, nM[b]	EC_{50} Shift x-Fold[c]	pA_2[d]
RFRP-3	1.17 ± 0.26		1		391.63 ± 44		1	
NPFF	11.95 ± 0.68				0.77 ± 0.19			
RF9	1163.50 ± 163	ND	4	5.75 ± 0.16	ND	383.27 ± 18.50	4	5.43 ± 0.04
GJ14	ND	21.08 ± 1.17	156	7.25 ± 0.09**,+	ND	387.37 ± 30.49	8	5.80 ± 0.03
GJ9	ND	210.75 ± 64.35	27	6.34 ± 0.14*,+	ND	366.77 ± 8.11	7	5.78 ± 0.10

Abbreviation: ND, not determined.

[a] Mean EC_{50} values for ligands that induce full receptor activation.

[b] Mean IC_{50} values for antagonists that fully reversed the agonist-induced receptor activation.

[c] Ratios with respect to the EC_{50} values of the agonist in the presence of the antagonist obtained from Gaddum/Schild EC_{50} shift equations. Fold shift = EC_{50} (agonist + compound)/EC_{50} (agonist).

[d] Values obtained from Gaddum/Schild EC_{50} shift equations. Comparisons of antagonist potency were made against RF9 at NPFF1R by one-way ANOVA followed by Dunnett's test (vs RF9, $*P < .05$, and $**P < .001$). Comparison between NPFF1R and NPFF2R were performed by unpaired *t* test ($+P < 0.05$, NPFF1R vs NPFF2R).

did not inhibit forskolin-induced cAMP production in NPY-Y1 overexpressing cells (Supplemental Figure 2, A and B). GJ14 did show very weak antagonism at the NPY-Y1 receptor, although only detectable at the highest concentration tested (Supplemental Figure 2C), almost 1000 times higher than the concentration required to antagonize RFRP-3 effects at NPFF1R. At KISS1R, GJ9 concentration dependently enhanced the binding of [^{125}I]kisspeptin-10 (Figure 3A), whereas all other tested compounds displayed no detectable affinity (Supplemental Table 1). Interestingly, RF9 showed competitive displacement activity at KISS1R (Figure 3A). Furthermore, RF9 alone induced IP1 accumulation on KISS1R-transfected HEK293 cells at approximately 10-fold less potency than the natural ligand, kisspeptin-10 (Figure 3B). Although GJ9 alone did not show agonism, both RF9 and GJ9 enhanced kisspeptin-10-induced IP1 accumulation (Figure 3C). GJ14 was void of any activity at KISS1R.

Experiment 2: RF9 but not GJ14 stimulates LH secretion via KISS1R

These results have shown for the first time that RF9 directly binds to and is an agonist at KISS1R. The kisspeptin receptor is renowned for mediating potent gonad-

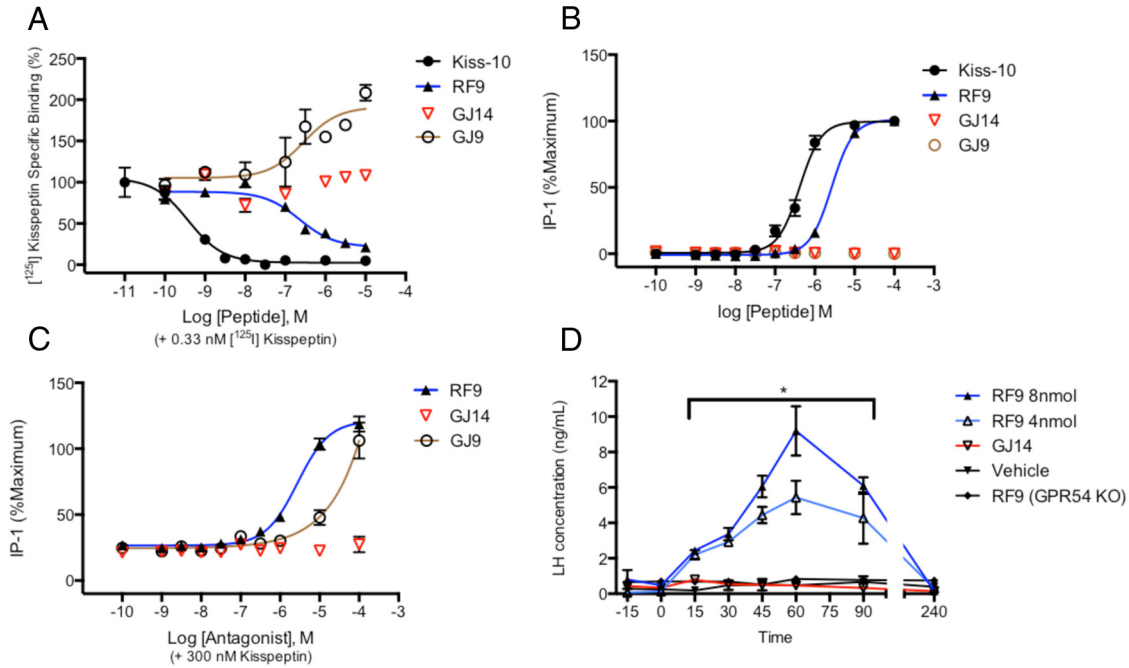

Figure 3. RF9 is a KISS1R agonist. Competitive displacement of [I^{125}]kisspeptin-10 binding profiles of representative ligands and test compounds at KISS1R (A) were performed in experiment 1a. Concentration-dependent production of agonist-induced IP1 accumulation in KISS1R-transfected HEK293 cells (B) were performed in experiment 1b. The effects of GJ9, GJ14, and RF9 on kisspeptin-10 induced IP1 accumulation (C) were performed in experiment 1b. RF9 and GJ14-induced LH release in diestrous wild-type or KISS1R-knockout mice (D) were performed in experiment 2.

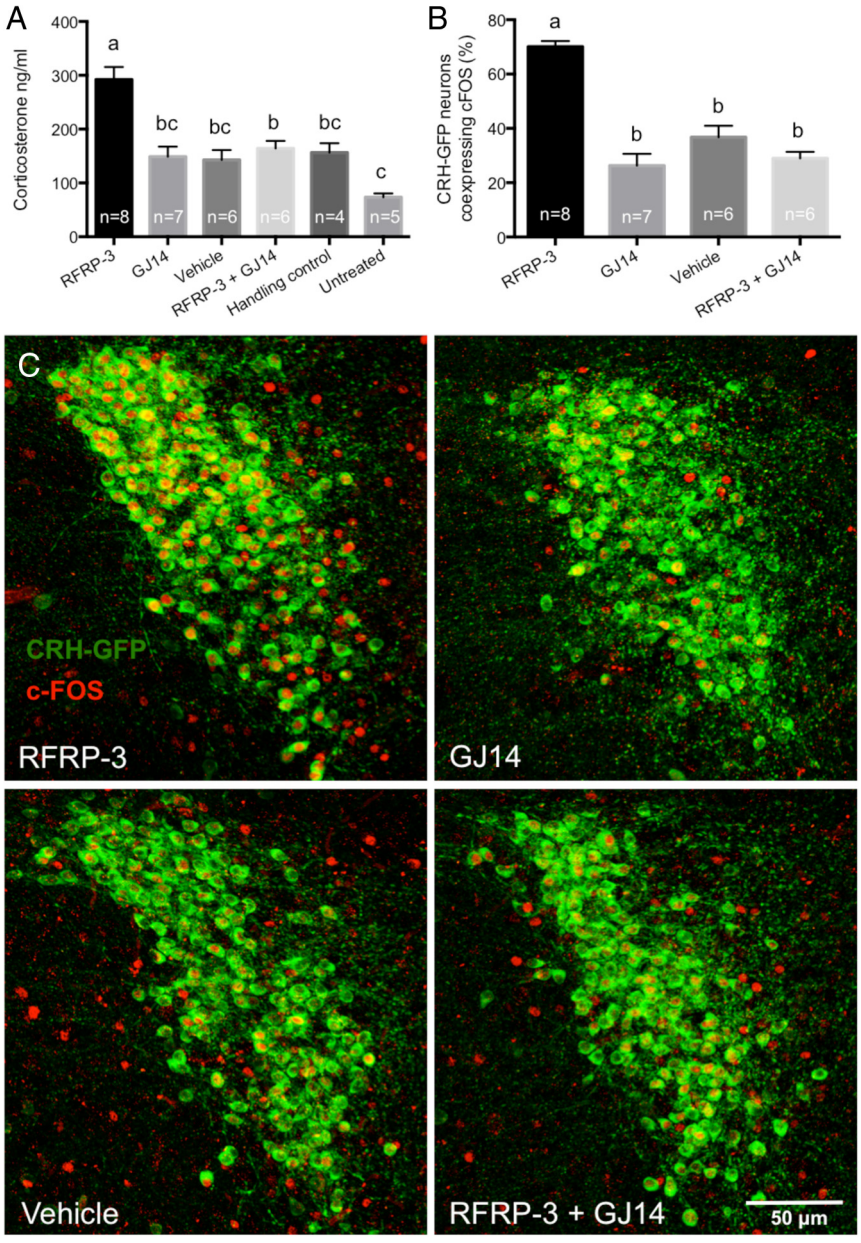

Figure 4. RFRP-3 is an activator of the HPA axis and is reversed with GJ14 (experiment 3). RFRP-3 induced corticosterone release and reversal with GJ14 in mice (A). B, Percentage of GFP-positive neurons coexpressing cFOS. C, Representative images of RFRP-3 induced cFOS expression in CRH-GFP neurons and reversal with GJ14. Groups with different letters in panels A and B are significantly different from each other ($P < .05$).

otropin release. In a strikingly similar fashion, RF9 has been shown to induce pronounced gonadotropin secretion in vivo (5–10). This has been attributed to a reversal of the inhibitory effects of RFRP-3 on GnRH neurons, which drive gonadotropin release. To test whether the blockade of NPFF1R indeed can cause such profound hypergonadotropic effects, we injected RF9 (4 or 8 nmol i.c.v.) or GJ14 (8 nmol i.c.v.) and took repeated tail blood samples for the measurement of LH concentration. As expected, injections of RF9 dose dependently increased circulating LH levels in diestrous female mice. In marked contrast, when diestrous mice were injected with GJ14, LH levels were unchanged (Figure 3D). Significantly, we report that RF9 (8 nmol i.c.v.) was completely unable to stimulate LH release in KISS1R KO mice, confirming a KISS1R-dependent mechanism of action.

Experiment 3: GJ14 prevents activation of the hypothalamic pituitary adrenal axis elicited by RFRP-3

The preceding experiments demonstrated that GJ14 is a potent and specific NPFF1R/2R antagonist in vitro. We next investigated whether GJ14 can antagonize the effects of RFRP-3 in vivo. CRH-GFP mice were injected i.c.v. with either RFRP-3 (3 nmol), GJ14 (30 nmol), RFRP-3 + GJ14, or vehicle. Acute i.c.v. injection of RFRP-3 significantly elevated circulating corticosterone levels compared with all groups ($P < .05$; Figure 4A). This stimulatory effect of RFRP-3 on the HPA axis was completely reversed by coadministration of GJ14. Colocalization of cFOS and CRH was measured using immunohistochemistry to confirm the activation of the CRH neurons by RFRP-3, which was again reversed by GJ14 cotreatment (Figure 4, B and C).

Experiment 4: chronic infusion of GJ14 reduces anxiety and reverses the anxiogenic effect of RFRP-3

RFRP-3-infused mice spent significantly less time in, and had less entries to, the light box compared with the vehicle-treated group ($P < .05$; Figure 5, C and D). Mice receiving GJ14 treatment alone spent significantly more time in the light box than vehicle controls ($P < .05$), presumably due to blockade of the anxiogenic effect of endogenous NPFF receptor agonists. The anxiogenic effect of RFRP-3 was completely reversed by cotreatment with GJ14. In the elevated plus maze, RFRP-3 infused mice spent significantly less time in the open arms of the elevated plus maze compared with GJ14-treated mice ($P < .05$; Figure 5E). Consistent with the blockade of RFRP-3 effects in the light-dark box, GJ14-cotreated mice spent significantly more time in the open arm compared with mice treated

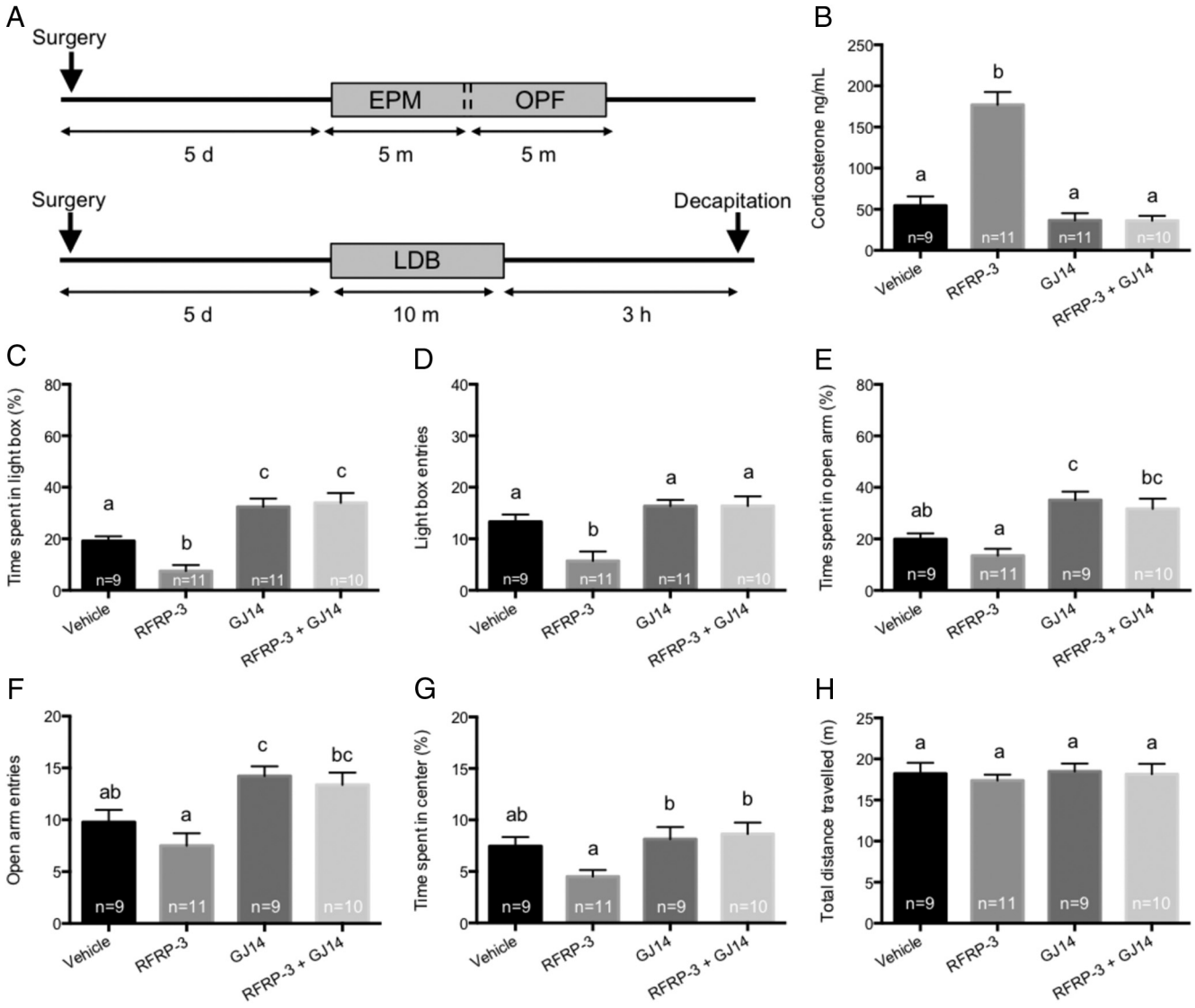

Figure 5. Chronic RFRP-3 infusion increases anxiety-like behavior and is reversed by the anxiolytic compound GJ14 (experiment 4). A, Experimental design for the behavioral testing. B, Basal circulating corticosterone levels are significantly higher in RFRP-3 infused mice. Percentage of time spent in light box (C) and number of light box entries (D) are shown. Percentage of time spent in the open arm of the elevated plus maze (E) and the number of open arm entries (F) are also shown. Percentage of time spent in the center of the open field (G) and total locomotion during open field test (H) are also shown. Groups with different letters are significantly different from each other ($P < .05$). EPM, elevated plus maze; OPF, open field; LDB, light dark box.

with RFRP-3 alone ($P < .05$; Figure 5E). This was consistent with the number of open arm entries (Figure 5F). In the open field test, RFRP-3-treated mice spent significantly less time in the center of the open field compared with both the GJ14 and RFRP-3 + GJ14 treated mice ($P < .05$; Figure 5G).

Collectively we provide evidence that RFRP-3 is an anxiogenic neuropeptide. Importantly, we also demonstrate that chronic blockade of the NPFF receptors using GJ14 has anxiolytic effects. These behavioral effects were not confounded by differences in locomotion because no differences in total distance traveled were observed during the open field test (Figure 5H). Circulating basal corticosterone levels in RFRP-3-treated mice were significantly higher than all other groups ($P < .05$; Figure 5B), suggesting that these mice were chronically exposed to high corticosterone levels throughout the infusion. This effect of RFRP-3 was completely abolished by cotreatment with GJ14.

Discussion

We report here that RFRP-3 is a potent HPA axis activator, inducing corticosterone release and causing anxiogenic responses. Furthermore, we have identified and

characterized a peptidic antagonist specifically targeting NPFF receptors, building on a previous report of NPFF receptor antagonism by this compound (28). Using this highly specific antagonist, we have established that blockade of the NPFF receptors is a novel anxiolytic target.

Surprisingly, RF9 was revealed to be an NPFF1R agonist in vitro. This was demonstrated using both cAMP and calcium mobilization experiments. RF9 displayed no NPFF1R antagonism at any concentration in both cAMP and calcium mobilization tests; therefore, our in vitro experiments indicate that achieving NPFF1R antagonism using RF9 in vivo would not be possible. Whereas RF9's agonism at NPFF1R was a surprising result, we note that Findeisen et al (24) have reported similar findings with RF9. To date, publications with pharmacological data demonstrating the function of RF9 at NPFF1R has been limited to Simonin et al (22) and Findeisen et al (24). Including our current work, there is now strong pharmacological evidence that RF9 is actually a weak, full NPFF1R agonist with other off-target effects, which further emphasizes the need for a true and selective NPFF1R antagonist.

Conversely, at the NPFF2R receptor, RF9, along with compounds GJ14 and GJ9, displayed antagonism at virtually equal potency. RF9 is therefore a suitable NPFF2R antagonist in vivo and indeed has been demonstrated to block the effects of NPFF (22). However, the use of RF9 is further limited by its agonism at KISS1R, which leads to its remarkably potent LH release (5–10, 35). Liu and Herbison (23) recently postulated that RF9's potent stimulatory effects on GnRH neuronal activity are KISS1R-mediated. Indeed RF9 had no effect on GnRH neuron firing rate in brain slice preparations from KISS1R-null adult mice. We report consistent findings in vivo as RF9 was completely without effect on circulating LH levels in KISS1R-null mice, confirming that the LH response to this compound is entirely dependent on kisspeptin receptor activation.

Taken together, we report the first direct evidence that RF9 binds to and activates KISS1R. These results clarify some confusion and controversy in the literature arising from use of RF9. In particular, interpretation of the marked hypergonadotropic effect of RF9 as being caused by blockade of a potent tonic inhibition of the reproductive axis by endogenous RFRP-3 (5–10) now appears to be misleading. Whereas indeed RFRP-3 can inhibit reproductive function, this suppressive effect is in fact rather mild (36) and thus seems inconsistent with the massive LH release induced by RF9. In contrast, GJ14, a potent and selective NPFFR antagonist, which does not act on KISS1R at the concentrations tested (up to 100 μM), did not elicit an LH release in diestrous female mice. There is currently debate as to whether RFRP neurons exert a hypophysiotropic action on pituitary gonadotrope cells via secretion of their neuropeptide the portal blood vessels or whether their reproductive effects are confined to the GnRH neuronal network (10). Because we administered GJ14 and RF9 centrally, the scope of experiment 2 is limited to central effects of these compounds.

Using GJ14, we were able to completely block the corticosterone release elicited by RFRP-3, thus validating the use of this compound in vivo. GJ14 also prevented the RFRP-3-induced induction of cFos in CRH-Cre-GFP neurons, which have been shown to reliably report 96% of immunoreactive CRH neurons (34). Alongside its activation of the CRH neurons, we report that RFRP-3 elicits anxiety-like effects when chronically infused. Our laboratory has observed similar anxiogenic responses to this neuropeptide in rats (M. Z. Rizwan and G.M.A., unpublished data). In mice, chronic infusion of GJ14 not only reversed the anxiogenic effect of RFRP-3 but also had anxiolytic-like properties compared with the vehicle-only controls. Elevated corticosterone levels imply that the anxiogenic effects of RFRP-3 are at least in part mediated by chronic hyperactivation of the HPA axis. Acute exposure to elevated corticosterone alone is sufficient to induce anxiety and cause dendritic hypertrophy in the basolateral amygdala (37). NPFF1R is broadly distributed in the brain but is particularly densely expressed in the PVN, brainstem, basolateral, central and medial amygdala, lateral septum, bed nucleus of stria terminalis, and ventral tegmental area (1, 10, 13, 38), all of which are known to play a role in the regulation of fear-, depression-, and/or anxiety-related behaviors. It is important to note that our behavioral studies come from female mice only, whereas the data for corticosterone measurements and CRH neuronal activation were for males. Our results may be applicable to both sexes, but caution should be exercised when generalizing the data to the opposite sex.

Recent reports have linked RFRP-3 and stress-induced infertility (11, 12). We conclude here that RFRP-3 itself is a stress- and anxiety-inducing neuropeptide. Our findings, combined with the known functions of RFRP-3 in the literature, present RFRP-3 in a new light. RFRP-3 expression has been shown to be up-regulated by stress (11, 12) and the following consequences could be surmised: further stimulation of CRH neurons, anxiety, and infertility. The reproductive suppression by RFRP-3 could also be indirectly exacerbated by its stimulation of CRH neurons, which are known to inhibit reproductive function (39–41). This activation of the HPA axis may also present an important potential confound to the past reproductive studies that needs to be considered. It would be important to study the effect of RFRP-3 on reproductive function, in

the absence its stimulation of CRH neurons, to dissect the true inhibitory effect of RFRP-3 on the reproductive axis.

The new NPFF receptor antagonist GJ14, with its superior potency, selectivity, and efficacy, will provide a much-needed accurate tool for studying the functions of the NPFF system in the future. Additionally, as RFRP-3 emerges as an important regulator of stress and anxiety responses, GJ14 and other modulators of NPFF receptors may hold therapeutic benefits, which remain to be explored in clinical settings.

Acknowledgments

We thank Dr Karl Iremonger for comments on an early draft of the manuscript and Professor Dave Grattan for his input throughout the project.

Address all correspondence and requests for reprints to: Joon Kim, Centre for Neuroendocrinology and Department of Anatomy, University of Otago School of Medical Sciences, PO Box 913, Dunedin 9054, New Zealand. E-mail: joon.kim.nz@gmail.com.

This work was funded by a University of Otago Research grant, University of Otago Priming Partnerships Pilot Project funding, and a Royal Society of New Zealand Marsden Grant.

Disclosure Summary: The authors have nothing to disclose.

References

1. **Liu Q, Guan X-M, Martin WJ, et al.** Identification and characterization of novel mammalian neuropeptide FF-like peptides that attenuate morphine-induced antinociception. *J Biol Chem*. 2001;276:36961–36969.
2. **Roumy M, Zajac J-M.** Neuropeptide FF, pain and analgesia. *Eur J Pharmacol*. 1998;345:1–11.
3. **Tsutsui K, Saigoh E, Ukena K, et al.** A novel avian hypothalamic peptide inhibiting gonadotropin release. *Biochem Biophys Res Commun*. 2000;275:661–667.
4. **Hinuma S, Shintani Y, Fukusumi S, et al.** New neuropeptides containing carboxy-terminal RFamide and their receptor in mammals. *Nat Cell Biol*. 2000;2:703–708.
5. **Bentley GE, Tsutsui K, Kriegsfeld LJ.** Recent studies of gonadotropin-inhibitory hormone (GnIH) in the mammalian hypothalamus, pituitary and gonads. *Brain Res*. 2010;1364:62–71.
6. **Glanowska KM, Burger LL, Moenter SM.** Development of gonadotropin-releasing hormone secretion and pituitary response. *J Neurosci*. 2014;34:15060–15069.
7. **Kriegsfeld LJ, Gibson EM, Williams W, et al.** The roles of RFamide-related peptide-3 in mammalian reproductive function and behaviour. *J Neuroendocrinol*. 2010;22:692–700.
8. **Pineda R, Garcia-Galiano D, Sanchez-Garrido M, et al.** Characterization of the potent gonadotropin-releasing activity of RF9, a selective antagonist of RF-amide-related peptides and neuropeptide FF receptors: physiological and pharmacological implications. *Endocrinology*. 2010;151:1902–1913.
9. **Pineda R, Garcia-Galiano D, Sanchez-Garrido MA, et al.** Characterization of the inhibitory roles of RFRP3, the mammalian ortholog of GnIH, in the control of gonadotropin secretion in the rat: in vivo and in vitro studies. *Am J Physiol Endocrinol Metab*. 2010;299:E39–E46.
10. **Rizwan MZ, Poling MC, Corr M, et al.** RFamide-related peptide-3 receptor gene expression in GnRH and kisspeptin neurons and GnRH-dependent mechanism of action. *Endocrinology*. 2012;153:3770–3779.
11. **Kirby ED, Geraghty AC, Ubuka T, Bentley GE, Kaufer D.** Stress increases putative gonadotropin inhibitory hormone and decreases luteinizing hormone in male rats. *Proc Natl Acad Sci USA*. 2009;106:11324–11329.
12. **Geraghty AC, Muroy SE, Zhao S, Bentley GE, Kriegsfeld LJ, Kaufer D.** Knockdown of hypothalamic RFRP3 prevents chronic stress-induced infertility and embryo resorption. *eLife*. 2015;4:e04316.
13. **Gouardères C, Kieffer BL, Zajac J-M.** Opposite alterations of NPFF1 and NPFF2 neuropeptide FF receptor density in the triple MOR/DOR/KOR-opioid receptor knockout mouse brains. *J Chem Neuroanat*. 2004;27:119–128.
14. **Vale W, Spiess J, Rivier C, Rivier J.** Characterization of a 41-residue ovine hypothalamic peptide that stimulates secretion of corticotropin and β-endorphin. *Science*. 1981;213:1394–1397.
15. **Griebel G, Holsboer F.** Neuropeptide receptor ligands as drugs for psychiatric diseases: the end of the beginning? *Nat Rev Drug Discov*. 2012;11:462–478.
16. **Griebel G, Holmes A.** 50 years of hurdles and hope in anxiolytic drug discovery. *Nat Rev Drug Discov*. 2013;12:667–687.
17. **Chalmers DT, Lovenberg T, De Souza E.** Localization of novel corticotropin-releasing factor receptor (CRF2) mRNA expression to specific subcortical nuclei in rat brain: comparison with CRF1 receptor mRNA expression. *J Neurosci*. 1995;15:6340–6350.
18. **Post A, Ohl F, Almeida OF, et al.** Identification of molecules potentially involved in mediating the in vivo actions of the corticotropin-releasing hormone receptor 1 antagonist, NBI30775 (R121919). *Psychopharmacology*. 2005;180:150–158.
19. **Smith GW, Aubry J-M, Dellu F, et al.** Corticotropin releasing factor receptor 1-deficient mice display decreased anxiety, impaired stress response, and aberrant neuroendocrine development. *Neuron*. 1998;20:1093–1102.
20. **Timpl P, Spanagel R, Sillaber I, et al.** Impaired stress response and reduced anxiety in mice lacking a functional corticotropin-releasing hormone receptor 1. *Nat Genet*. 1998;19:162–166.
21. **Kaewwongse M, Takayanagi Y, Onaka T.** Effects of RFamide-related peptide (RFRP)-1 and RFRP-3 on oxytocin release and anxiety-related behaviour in rats. *J Neuroendocrinol*. 2011;23:20–27.
22. **Simonin F, Schmitt M, Laulin J-P, et al.** RF9, a potent and selective neuropeptide FF receptor antagonist, prevents opioid-induced tolerance associated with hyperalgesia. *Proc Natl Acad Sci USA*. 2006;103:466–471.
23. **Liu X, Herbison AE.** RF9 excitation of GnRH neurons is dependent upon kiss1r in the adult male and female mouse. *Endocrinology*. 2014;155:4915–4924.
24. **Findeisen M, Wu¨rker Cc, Rathmann D, et al.** Selective mode of action of guanidine-containing non-peptides at human NPFF receptors. *J Med Chem*. 2012;55:6124–6136.
25. **Maletínská L, Tichá A, Nagelová V, et al.** Neuropeptide FF analog RF9 is not an antagonist of NPFF receptor and decreases food intake in mice after its central and peripheral administration. *Brain Res*. 2013;1498:33–40.
26. **Rudolf K, Eberlein W, Engel W, et al.** The first highly potent and selective non-peptide neuropeptide Y Y 1 receptor antagonist: BIBP3226. *Eur J Pharmacol*. 1994;271:R11–R13.
27. **Aiglstorfer I, Hendrich I, Moser C, Bernhardt G, Dove S, Buschauer A.** Structure-activity relationships of neuropeptide YY 1 receptor antagonists related to BIBP 3226. *Bioorg Med Chem Lett*. 2000;10:1597–1600.
28. **Mollereau C, Mazarguil H, Quelven I, et al.** Pharmacological characterization of human NPFF(1) and NPFF(2) receptors expressed in

CHO cells by using NPY(1) receptor antagonists. *Eur J Pharmacol*. 2002;451:245–256.
29. **Mollereau C, Gouardères C, Dumont Y, et al.** Agonist and antagonist activities on human NPFF2 receptors of the NPY ligands GR231118 and BIBP3226. *Br J Pharmacol*. 2001;133:1–4.
30. **Beltramo M, Robert V, Galibert M, et al.** Rational design of triazolo-lipopeptides analogs of kisspeptin inducing a long-lasting increase of gonadotropins. *J Med Chem*. 2015;58(8):3459–3470.
31. **Steyn F, Wan Y, Clarkson J, Veldhuis J, Herbison A, Chen C.** Development of a methodology for and assessment of pulsatile luteinizing hormone secretion in juvenile and adult male mice. *Endocrinology*. 2013;154:4939–4945.
32. **García-Galiano D, van Ingen Schenau D, Leon S, et al.** Kisspeptin signaling is indispensable for neurokinin B, but not glutamate, stimulation of gonadotropin secretion in mice. *Endocrinology*. 2011; 153:316–328.
33. **Taniguchi H, He M, Wu P, et al.** A resource of Cre driver lines for genetic targeting of GABAergic neurons in cerebral cortex. *Neuron*. 2011;71:995–1013.
34. **Wamsteeker Cusulin JIW, Füzesi T, Watts AG, Bains JS.** Characterization of corticotropin-releasing hormone neurons in the paraventricular nucleus of the hypothalamus of Crh-IRES-Cre mutant mice. *PLoS One*. 2013;8:e64943.
35. **Caraty A, Blomenröhr M, Vogel G, Lomet D, Briant C, Beltramo M.** RF9 powerfully stimulates gonadotrophin secretion in the ewe: evidence for a seasonal threshold of sensitivity. *J Neuroendocrinol*. 2012;24:725–736.
36. **Ducret E, Anderson GM, Herbison AE.** RFamide-related peptide-3, a mammalian gonadotropin-inhibitory hormone ortholog, regulates gonadotropin-releasing hormone neuron firing in the mouse. *Endocrinology*. 2009;150:2799–2804.
37. **Mitra R, Sapolsky RM.** Acute corticosterone treatment is sufficient to induce anxiety and amygdaloid dendritic hypertrophy. *Proc Natl Acad Sci USA*. 2008;105:5573–5578.
38. **Wu C-H, Tao P-L, Huang EY-K.** Distribution of neuropeptide FF (NPFF) receptors in correlation with morphine-induced reward in the rat brain. *Peptides* 2010;31:1374–1382.
39. **Petraglia F, Sutton S, Vale W, Plotsky P.** Corticotropin-releasing factor decreases plasma luteinizing hormone levels in female rats by inhibiting gonadotropin-releasing hormone release into hypophysial-portal circulation. *Endocrinology*. 1987;120:1083–1088.
40. **Rivest S, Plotsky P, Rivier C.** CRF alters the infundibular LHRH secretory system from the medial preoptic area of female rats: possible involvement of opioid receptors. *Neuroendocrinology*. 1993; 57:236–246.
41. **Rivier C, Vale W.** Influence of corticotropin-releasing factor on reproductive functions in the rat. *Endocrinology*. 1984;114:914–921.